



A H2020 Research and Innovation Action project, Grant Agreement number 814985

D6.3 – Detailed engineering design package



This Deliverable 6.3 report is part of a project that has received funding from the European Union's Horizon 2020 research and innovation program under grant agreement No. 814985

WP 6: Test Rig and experimental validation

Task 6.3: Dynamic simulation report

Version: Final, Wednesday, 29 September 2021

Technical References

Deliverable No.	6.3
Dissemination level ¹	Confidential
Work Package	6: Test Rig and experimental validation
Task	6.3: Dynamic simulation report
Lead beneficiary	TU Wien
Contributing beneficiary(ies)	/
Due date of deliverable	09/30/2021
Actual submission date	09/29/2021

¹ PU = Public
 PP = Restricted to other program participants (including the Commission Services)
 RE = Restricted to a group specified by the consortium (including the Commission Services)
 CO = Confidential, only for members of the consortium (including the Commission Services)

History of Changes

Version	Date	Changes
1	09/28/2021	Viktoria ILLYÉS and Andreas WERNER
2	09/29/2021	Implemented minor suggestions by Giampaolo Manzolini
Final	09/29/2021	Approved by Giampaolo Manzolini

Disclaimer

This document contains proprietary information of the SCARABEUS project.

All rights reserved.

Copying of (parts) of this document is prohibited without prior permission in writing.

Executive Summary

Dynamic modeling of sCO₂-cycles connected to fluctuating energy sources or sinks is key for making statements about the performance. The simulation software APROS (**A**dvanced **P**rocess **S**imulator) provides the necessary standard components and a control structure for simulating industrial-sized power cycles.

In SCARABEUS, as a first step, the test rig was modelled in its current modification “Mod1”. Experiments to look at are heat transfer measurements for which the whole test rig needs to be in operation anyway.

For CO₂, APROS only provides the so-called 3-equation model, which does not treat vapor and liquid in the 2-phase region separately like it does with water systems but as a mixed property single phase.

Heat transfer implementation showed atypical behavior for CO₂. User-defined correlations for the heat transfer have been implemented, and experiments for cooling and condensing have been performed.

Future work will be performed on comparing the results from our actual heat transfer measurement campaign to the simulation’s results. Based on this analysis the authors will publish a final statement whether APROS is a suitable tool for simulating sCO₂ cycles.

Table of Contents

Executive Summary	4
Table of Contents	5
Introduction	6
1 Dynamic Process Simulation with CO ₂ – Brief Literature Overview	6
APROS (Advanced Process Simulator).....	7
2 How does APROS work	7
2.1 Six Equation Model and Three Equation Model.....	7
2.2 Definition of fluids.....	9
2.3 Modeling of components	9
Simulation and results	11
3 Scope of Simulation	11
3.1 Scope	11
3.2 Process control.....	12
4 Heat transfer calculation	13
4.1 Preset calculation of the heat transfer coefficient for condensation	13
4.2 Methods for implementing your equations for calculating the htc.....	16
5 Results.....	19
5.1 Studying the calculation of heat transfer	19
5.2 Modelling Mod1 test rig - cooling experiments	19
5.3 Modelling Mod1 test rig - condensing experiments	20
5.4 Finding control parameters to use as a guess for actual operation and determine the most efficient order of experiments.....	21
5.5 See the influence of water in comparison to coolant (35% MEG) in case the TU Wien building department switches operation without giving notice.....	21
5.6 Determine how long it takes to reach thermodynamic equilibrium.....	22
5.7 Modeling of CO ₂ with RP or EP.....	23
Summary and Conclusion	24
Literature.....	25

Introduction

1 Dynamic Process Simulation with CO₂ – Brief Literature Overview

When implementing fluctuating heat sources from renewable energy or waste heat and heat sinks influenced by the weather, it can be helpful to know the system's dynamic performance. For a test rig like ours, dynamic simulation (even if only parts of the system can be modelled) provides valuable insight into the process and operation of the test rig and possible challenges that might occur.

From our Institute's experience in simulating industrial water/steam cycles, APROS seemed the tool of choice for our research questions.

The review paper of Wang et al. [1] provides an overview of used software or code for the dynamic simulation of supercritical CO₂ Brayton cycles.

Table 1: The overall details of worldwide simulation researches of supercritical Brayton cycles, [1]

Institution	Layout	Software/Code	Heat exchanger Recuperator: R; Heater: H; Cooler: C	Turbomachines	Application object
Echogen [22]	Layout 2	GT-SUITE	R and C: PHE	TG-TC	–
MIT [23,24]	Layout 4, Layout 2	GAS-PASS; Fortran90	PCHE	TAC	Nuclear
BMPC [25]	Layout 2	TRACE	H: STHE	TG-TC	–
NNL [26]	Layout 2	TRACE	C: STHE	TG-TC	–
SNL [27]	Layout 1	Simulink	C:STHE	TAC	Nuclear
XJTU [28,29]	Layout 4/ Layout 2	Simulink/ SCTran	R and C: PCHE	TG-C/TAC	Nuclear
HEU [30]	Layout 4	RELAP5	PCHE	TAC	Nuclear
TRCF [31]	Layout 2	Apros	R and C: PHE	TG-C	Solar power
BMPC/KAPL [32]	Layout 4/ Layout 2	Modified TRACE	–	TAC	Nuclear
TPG [33]	Layout 4	Simulink	R: STHE	TG-C	Coal
USYD [34,35]	Layout 4	Dymola;	PCHE	TAC	Solar power
ANL [36]	Layout 4/ Layout 2	PDC	H: STHE R: PCHE	TAC	Nuclear
Sheffield Univ. [37]	Layout 3	Simulink	PCHE	TAC	Industrial
KAERI [38]	Layout 1	MARS	PCHE	TG-C	Nuclear
UQ [40]	Layout 2	Dymola	–	TAC	Solar power
KAIST [41]	Layout 2	GAMMA+	R: PCHE	TAC	Nuclear
EDF R&D [42]	Layout 4	Dymola	R: PCHE	TG-C	Solar power
NETL [43]	Layout 4	Aspen Plus Dynamics	R: PCHE	TG-C	Fossil-fuel power
Brunel University [44]	Layout 2	GT-SUITE	H: MTHE; R: PCHE; C: PHE	TAC	Waste heat recovery
GE [45]	Layout 2	NPSS	R and C: PCHE	TG-C	Natural gas

[1] PHE: Plate heat exchanger
[2] STHE: Shell-and-tube heat exchanger
[3] PCHE: Printed circuit heat Exchanger
[4] MTHE: micro-tube heat exchangers
[5] MIT: Massachusetts Institute of Technology
[6] BMPC: Bechtel Marine Propulsion Corporation
[7] NNL: Naval Nuclear Laboratory
[8] SNL: Sandia National Laboratory
[9] XJTU: Xi'an Jiaotong University
[10] HEU: Harbin Engineering University
[11] TRCF: Technical Research center of Finland
[12] KAPL: Knolls Atomic Power Laboratory
[13] TPG: Thermal Power Group
[14] NETL: National Energy Technology Laboratory
[15] USYD: The University of Sydney
[16] ANL: Argonne National Laboratory
[17] KAERI: Korea Atomic Energy Research Institute
[18] UQ: The University of Queensland
[19] KAIST: Korea Advanced Institute of Science and Technology
[20] GE: General Electric Co.

APROS (Advanced Process Simulator)

APROS stands for "Advanced Process Simulator" and has been developed by VTT (Technical Research Centre of Finland) and Fortum since the late 1980s.

2 How does APROS work

Although APROS is quite common in simulations of industrial water/steam-cycles, its documentation is scientific oriented presupposing know-how about the models being available.

2.1 Six Equation Model and Three Equation Model

APROS provides a total of six different thermal-hydraulic models, three of which are suitable for describing one-dimensional flow of liquid and steam. The most powerful of these models is the so-called 6-equation system used for water/steam-systems since it applies the three conservation laws to the phases in the wet steam region separately. APROS couples these equations with empirical correlations describing various phenomena in the two-phase region, such as heat transfer and friction at the phase boundary. However, the 6-equation model is limited to certain fluids, specified by so-called "sections".

When using carbon dioxide as a working fluid, the program only allows for the homogeneous flow model (also called the 3-equation model). It applies the three conservation laws to the mixture in the two-phase region, thus, not considering the two phases separately. Accordingly, the properties such as temperature or flow velocities are calculated for a so-to-say single phase made up of liquid and gas by averaging over the flow cross-section.

The three one-dimensional differential equations for the conservation of mass (1), momentum (2), and energy (3) are defined in the APROS documentation for the homogeneous model as follows:

$$\frac{\partial(A\rho)}{\partial t} + \frac{\partial(A\rho v)}{\partial z} = S_M \quad (1)$$

$$\frac{\partial(A\rho v)}{\partial t} + \frac{\partial(A\rho v^2)}{\partial z} + \frac{\partial(Ap)}{\partial z} = S_I \quad (2)$$

$$\frac{\partial(A\rho h)}{\partial t} + \frac{\partial(A\rho h v)}{\partial z} = S_E \quad (3)$$

A stands for the flow cross-section, ρ for the density, p for the pressure, v for the flow velocity, and h for the total specific enthalpy, including kinetic energy $v^2/2$. The terms are derived according to the time t and the coordinate z , which describes the fluid flow. The last term „ S “ in each of the three equations stands for the mass, momentum, and energy source term. S_M may include the additional mass flows introduced into the system. S_I can consist of pressure losses

due to friction, hydrostatic pressure differences, and the pressure increase due to the pump. In contrast, S_E can consist of the energy losses due to friction, heat flows, and the derivative of pressure with respect to time.

The derivative of pressure is listed in the source term of equation (3) since enthalpy is used instead of internal energy:

$$\frac{\partial u}{\partial t} = \frac{\partial h}{\partial t} - v \frac{\partial p}{\partial t} \quad (4)$$

Equation (4) is documented in [2] without the specific volume "v". This is not correct due to unit nomenclature, so the equation is taken from paper [3]. It deals with an add-on package for APROS, using a simplified form of the homogeneous model calculation, but has no further relevance to this work except for this formula. u is the specific internal energy, v is the specific volume, and p is the pressure.

In paper [4], which deals with the codes of dynamic process simulations, and in the thesis in collaboration with VTT [5] on simulations at supercritical pressures with APROS, the value of zero is given for S_M . The conservation laws for the 6-equation system and the homogeneous model are essentially the same.

The heat conduction in pipe walls is calculated in the cylindrical coordinate system according to equation (5):

$$\rho c_p \frac{\partial T}{\partial t} = \frac{1}{r} \frac{\partial}{\partial r} \left(r \lambda \frac{\partial T}{\partial r} \right) + Q' \quad (5)$$

Q' stands for heat flux per unit volume and t for time. T , λ , ρ and c_p are the solid material's temperature, thermal conductivity, density, and specific heat capacity. r is the radius in the direction of the coordinate axes.

To solve the conservation laws numerically, one must discretize them for space and time. The spatial discretization of the thermal-hydraulic system is done according to the "staggered grid" principle by calculating the state variables (e. g. pressure) in the middle of a node and the flow variables (e. g. mass flow) in the connection between two nodes, also called bifurcation. The calculation of heat conduction is discretized according to the same principle and is subsequently applied to the calculation of temperatures in the pipes. This temperature is used to calculate the remaining properties of the solid material via material functions.

For one-dimensional heat conduction and homogeneous two-phase flow, an implicit solution algorithm is used to calculate the systems of equations for pressure and enthalpy, and the pipe wall temperatures. However, an implicit solution is not possible coupling these systems of state equations with the properties of the medium and heat transfer calculation. Thus, an iterative procedure must be used to calculate the whole system. In this case, the iteration steps are carried out as often as necessary until the solution converges. The implicit Euler method is used for the integration. The nonlinear terms of conservation equations and the correlation of heat conduction are linearized, ensuring the simulation's convergence. Thereby, especially in the source terms, strongly nonlinear quantities are present.

2.2 Definition of fluids

The fluids are implemented in the model by so-called "sections", in which fluids or fluid components of a mixture are added or removed depending on specific databases. Consequently, only substances available in these databases can be processed.

Two possible sections are available, in which the CO₂ circulating in the main circuit is already predefined. Two databases have CO₂ predefined among other substances: "RP" and "EP". CO₂ is specified by number: 6 for "EP" and 9 for "RP". "RP" differs from other sections as it uses the external software NIST Refprop. For CO₂, the same equation of state from [6] is applied by both options, which is expressed in terms of Helmholtz energy using temperature and density and is defined as follows:

$$\frac{E_H(\rho, T)}{RT} = \Phi_H(\delta, \tau) = \Phi_H^0(\rho_r, \tau_r) + \Phi_H^r(\rho_r, \tau_r) \quad (6)$$

E_H represents the specific and Φ_H the dimensionless Helmholtz energy. Φ_H is split into a part Φ_H^0 which considers the ideal gas behavior and a part Φ_H^r which considers the residual fluid behavior. ρ_r is the reduced density at a critical state value of 467.6 kg/m³, while τ_r is the inverse reduced temperature and R is the specific gas constant. By combining derivatives of equation (6), all thermodynamic properties of a pure fluid can be calculated. The correlation is valid for states from the triple point to temperatures and pressures of 1100 K and 880 bar. For the maximum temperatures and pressures of the experiments discussed in this paper (180 °C and 66 bar), the maximum uncertainties of the correlation for density and specific isobaric heat capacity are ±0.05% and ±0.15%, respectively.

2.3 Modeling of components

The model has been completely assembled from standard process components while adjusting these prefabricated modules via their properties to better fit the real component's properties. The necessary data are all taken from technical data sheets or drawings. The experiments run via codes written in SCL (Simantics Constraint Language), a variant of the Haskell programming language.

For the visual components, graphical symbols are available that can be dragged onto a workspace (called a "diagram" in APROS) and linked there using signals. The components (and also the workspaces) can be divided into three categories: Process, Automation, and Generic components. With the help of the process components the actual process is modeled. These include components designed to represent a specific real component, covering an enormous range of components, from pipe sections to pumps to heat exchangers or throttles.

On the other hand, so-called "point" and "node" modules can be used. The "Points" are used as an interface between the other process components since these cannot be connected directly to their signals. "Nodes" allow for the same functionality but are more versatile because a volume can be entered directly in their properties, whereas the "Point" modules get their volume from the adjacent components. In addition, "Nodes" have multiple connection points and can be used to create one's non-standard process components, such as a tank.

The program is operated and built using modules available as standard, which are primarily divided into visual and non-visual components. For example, in the non-visual components, the properties of solid materials and fluids can be viewed and manipulated. Additionally, there is the option to model an own medium, e.g. to create a special coolant. Furthermore, it is possible to transfer external data into the simulation model and to export results from the model.

Each process component possesses a substructure: the computation level. This level consists of a diversity of further modules, which are declared in this work as computation components since they execute the actual computation of the process component and consist of computation nodes and their connections ("branches"). Accordingly, this substructure forms the spatial discretization mentioned in the previous chapter. A large part of the parameters is visible and changeable only on this level.

This substructure differentiates the individual process components by using different computation components from each other and lends thereby their individuality. While the calculation level of a simple pipe section is built only from thermo-hydraulic calculation nodes and concentration modules (abbreviated with TB and KM), as well as their connections to each other, the substructure of a heat exchanger component consists additionally of some more components: the heat transfer module (WM), as well as the inner and outer calculation nodes of the heat structure (BW) and their connections to each other. The discretization of these two process components, which are connected by a "point" module, is shown in Figure 1.

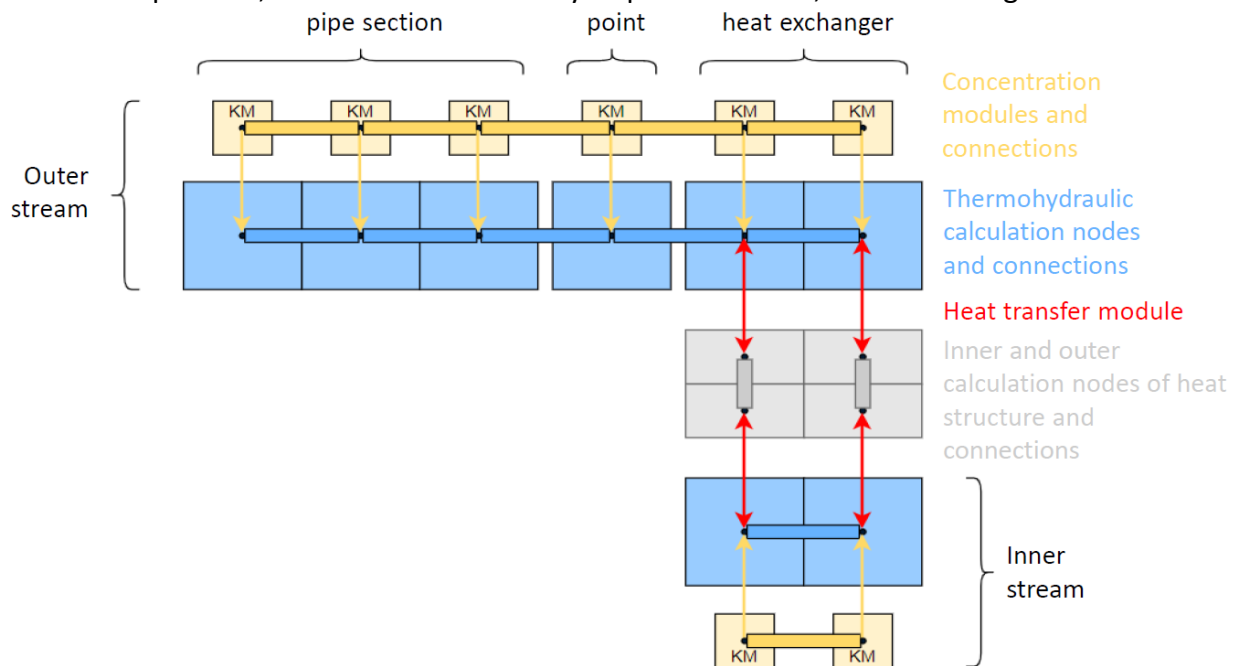


Figure 1: Discretization of a piping and heat exchanger component connected via a "Point", adapted from [7]

In the TB, which represent the internal volume of a pipe, the state variables such as pressure and enthalpy are calculated. These nodes are axially linked via the thermo-hydraulic branches, where the flow variables, such as mass flow, are determined. The selected "section" is anchored in the TB.

The KM are implemented by the program itself, depending on the selected SECTION and store both the chemical composition of the fluids and the composition of the liquid and vapor

phase in mass fractions. In these calculation components, the material properties are solved depending on the pressures, enthalpies and mass fractions obtained from the TB. The CMs are axially linked to each other through their connections. Furthermore, each concentration module is connected to its corresponding TB, thus forming a parallel grid with the thermo-hydraulic network.

The BW define the inner and outer surfaces of the pipe walls involved in heat transfer and determine the related wall temperatures for the entire perimeter. These calculation nodes are radially linked to the corresponding connection, which performs the calculation of heat conduction through the solid structure. Although it is possible to create axial connections between the individual BW, this option is not used. In this case, the heat transfer modules represent the connecting link between the BW and the TB. In this calculation component, the heat transfer coefficient α is calculated.

With the heat transfer coefficient α , the heat flux density \dot{q} between a pipe wall and the fluid can be calculated according to equation (7), with the help of the temperatures of the calculation nodes of the thermal hydraulic and thermal structure system T_{TB} and T_{BW} .

$$\dot{q} = \alpha(T_{BW} - T_{TB}) \quad (7)$$

Simulation and results

3 Scope of Simulation

3.1 Scope

The scope of the simulation included:

- Studying possibilities to model components of Mod1 test rig
- Studying the calculation of heat transfer
- Implementing a user-defined heat transfer correlation
- Modeling Mod1 test rig as a closed cycle, see Figure 2
 - For heat transfer measurements for cooling and condensing CO₂

- In the test tube, the mass flow of the cooling liquid is directly regulated.
- The rotation speed of the pump regulates the CO₂ mass flow in the main circuit.
- The mass flow of the thermal oil is regulated via the pressure difference of the thermal oil side inlet and outlet.
- The throttle of the main circuit regulates the pressure in the high-pressure section.

The parameters are adjusted with a PID-controller and an actuator. If the variable can be adjusted purely by manipulating a boundary value, as in the case of the precooler input temperature, only one controller is sufficient. Suppose this is impossible and an additional component like a valve or the pump is required for control. In that case, an additional actuator is connected between the controlled component and the controller.

4 Heat transfer calculation

4.1 Preset calculation of the heat transfer coefficient for condensation

The basic equations pre-implemented in APROS for calculating the heat transfer coefficient (htc) are selected considering the fluid/wall temperature difference and the states in the thermo-hydraulic calculation node. Single-phase heat transfer, evaporation, and condensation are treated differently.

For single-phase forced convection, the Dittus-Boelter relation presented in equation (8) is used:

$$\alpha_{DB} = 0,023 \left(\frac{\lambda}{D_i} \right) Pr^{0,4} Re^{0,8} \quad (8)$$

According to [8], the power of the Prandtl number should be 0.3 when cooling the medium and 0.4 when heating it, but no consideration is given to this in the APROS calculation.

For bubble and boiling evaporation, the Chen relationship (9) is used, which is a combination with equations (10) and (11) and is designed for vertical, stable two-phase flows.

Equation (10) consists of the Dittus-Boelter correlation α_{DB} defined in equation (8) multiplied by the Reynolds number function F , which is the ratio of the Reynolds number for the mixture and the liquid fraction. F is solved either empirically or via a momentum transfer analogy. In the literature, α_{DB} is defined for the pure liquid phase [25], but this definition is not present in the APROS documentation [9].

In equation (11), the parameter Su is defined as an empirically determined "suppression" factor, and ΔT_s is defined as the difference between the wall and saturation temperatures. Δp is the difference in vapor pressure corresponding to ΔT_s . The exact definitions, as well as calculations of F and Su , are given in [9].

(9)

$$\alpha_{Chen} = \alpha_1 + \alpha_2$$

(10)

$$\alpha_1 = \alpha_{DB} F$$

$$\alpha_2 = 0,00122 \frac{\lambda_f^{0,79} c p_f^{0,45} \rho_f^{0,49}}{\sigma^{0,5} \mu_f^{0,29} h_v^{0,24} \rho_d^{0,24}} \Delta T_S^{0,24} \Delta p^{0,75} S u \quad (11)$$

For condensation, equation (12) is given in the APROS documentation:

$$\alpha_{\text{Kon,lam}} = 0,296 \left[\frac{\rho_f(\rho_f - \rho_d) g h_v' \lambda_f^3}{D_c \mu_f (T_G - T_{\text{Wa}})} \right]^{0,25} \quad (12)$$

The equation is valid for stratified flows in a horizontal pipe at low flow velocities of the steam and low shear forces at the boundary layer [10]. This statement contradicts the application in the program since it is assumed that the two-phase flow is homogeneous, and this assumption is valid only at high flow velocities, [2].

The only point to be emphasized here is, that it is not clear from the literature whether the quantities with the indices liquid and vapor are values related to the saturation state or specifically to the conditions of the individual phases. However, since APROS makes no distinction between the two phases even when calculating the temperature and averages the properties over the cross-section and since the temperature in the two-phase region depends only on the saturation pressure, it is assumed that the saturation temperature sufficiently defines the state. Furthermore, for the characteristic diameter, the assumption is made here that it is the inner diameter.

Since the simulation results at preset do not agree with the general behavior of condensation of CO₂ from several papers, manual calculations using equation (12) for a single thermohydraulic calculation node (node 51 of 100) of the test tube have been performed. These calculations were performed using saturation and mixing values from the software, as well as saturation values from NIST Refprop.

Two "point" modules were created for pure vapor and pure liquid to obtain the saturation values. These nodes were connected to the process component of a pipe; otherwise, no values would be output at the calculation level after starting the simulation. In addition, both nodes were excluded from the simulation so that the variables are declared as boundary values and are not variable by other processes. The results of the manual calculation with these saturation parameters from the software hardly changed over the condensation process and amounted to a minimum and maximum values between 610 and 640 W/(m²K).

For the calculation with mixed fluid values, the parameters of specific heat capacity, dynamic viscosity, and thermal conductivity were plotted from the associated TB for different vapor contents, as shown in Figure 3 and inserted in equation (12). The difference in density for the pure vapor and liquid states was left at saturated values since inserting the mixed values would yield a result of zero. The results change only marginally from those with saturation values because the parameters have little effect on the results due to the opposite slope or slope down. With the saturation values from NIST Refprop Version 9.1, the results are slightly lower than the two calculations above because the specific heat capacities from the database used are lower. However, the general behavior remains the same. There is a considerable difference between the values from the simulation and the manual calculations for all three calculation methods.

When calculated with both saturation and mixing values, the results obtained for the entry into the condensation phase are not far from the simulation results. Based on this fact, it is

hypothesized that equation (12) is not fully specified in the APROS documentation and either an additive or multiplicative factor is added to the relationship. The application of the same principle in the calculation of evaporation and the steady slope of the heat transfer coefficient (visualized in Figure 3), further strengthens this assumption.

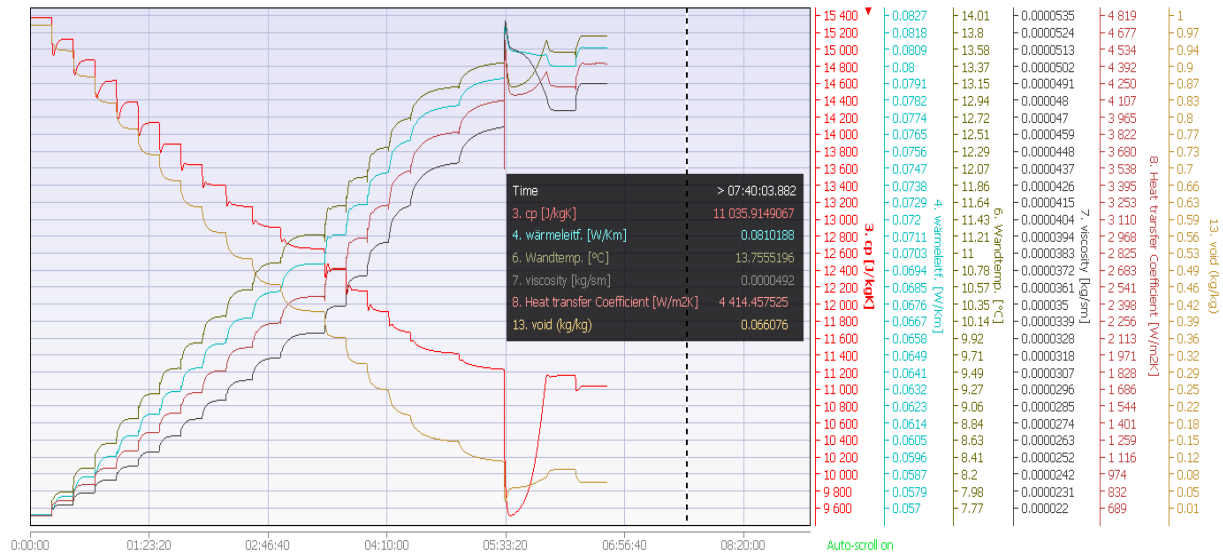


Figure 3: Diagram of mixing parameters of the calculation node 51 of the test tube

As a further hypothesis, it is suggested that the term is related to the vapor content as well as the Reynolds- and Prandtl-numbers. Therefore, a multiplicative factor is ruled out. If the first assumption is reliable, it would have to take the value of one at the beginning of condensation. It is unclear how the relationship with the above factors should arise.

Thus, the assumption of applying an additive factor is evaluated as more probable here. This additive term is, in all likelihood, equation (6), weighted by water content since the Dittus-Boelter equation is also used for evaporation, and this would represent the turbulent part of the equation. The vapor content additionally weights the component of equation (12).

Therefore, a literature search was conducted with the goal of finding an equation that reflects the result of the simulation. Since none of these equations met the necessary requirements, they are not further listed.

It appears that equation (12) given in the APROS documentation is only part of the correlation used to calculate the heat transfer coefficient for condensation. Via trial and error and consultation with the ASPEN-support, the complete equation (13) could be obtained:

$$\alpha_{\text{Kon,lam,A}} = (1 - \beta)\alpha_{\text{DB}} + \alpha_{\text{Kon,lam}}\beta \quad (13)$$

$$\beta = \frac{x - a}{1 - a} \quad (14)$$

The equation refers to a zone described as a "wet wall". Here, the factor β , shown in equation (14), is not the pure vapor content but a smoothing coefficient into which the vapor content enters and which is used to weigh the two terms in equation (13).

Three different approaches to cope with this formula were considered and discussed even with the support:

- Proposal from support: assigning a substantial negative value to the constant
 - Therefore, only $\alpha_{kon,lam,A}$ is now considered in the calculation.
 - This approach is not useful because the heat transfer coefficient, regardless of efficiencies, would increase as the steam coefficient decreases.
- Assigning a value approaching one (but not one)
 - Otherwise, it will be divided by the value zero and the calculation of the program will diverge. Thus, after a short transition phase at the beginning of the condensation, only the component α_{DB} is considered. The positive aspect of this method is the descending behavior of the heat transfer coefficient with the vapor content, which can be corrected up or down with the efficiency of the heat exchanger.
 - However, this method is too crude and simplistic to represent the real behavior of condensation.
- Create a custom function for the constant, either via automation or via SCL code
 - The problem with this is that the constant always needs to be very close to the vapor content, especially at the beginning of the condensation, to get results. In addition, the smoothing coefficient can only move between the values zero and one. Thus, the effect is limited and this creates the need to work with the efficiency of the process component of the heat exchanger. This would make the practical implementation extremely complex.

Finally, it was decided to disable the heat transfer coefficient calculation during condensation within the software and to find a way to implement a custom equation.

4.2 Methods for implementing your equations for calculating the htc

There are generally three approaches to building in a custom equation, neglecting the pre-implemented equation for condensation:

- building a calculation component purely with standard components,
- building an SCL- based user component,
- and the "External Automation" module.

In the first case, the equation is represented with an automation composed only with the help of components, which are available in APROS from the beginning. In total, the structure consists of measurement and calculation components, an element for inserting constant values, and the transmission component called "Value Transmitter". With the help of these components, the necessary parameters are taken from the process, utilized, and fed back into the desired component.

The "Value Transmitter" must be used to feed the calculated variable into the heat transfer module, as the component is able to utilize analog signals and overwrite the desired attribute with this analog value. The module can also be used to measure parameters, which are then available as analog values.

The component has an attribute that allows defining the simulation phase at which the signals are evaluated. Taking values via "Value Transmitter" should generally be done at the beginning of the simulation time step, as this procedure achieves the best results. This was empirically determined by mapping the Dittus-Boelter correlation according to equation (6) using automation and comparing the calculated values with those of the standard calculation in APROS. Figure 4 visualizes this method, whose structure consists of two parts. The first part consists of calculating the heat transfer coefficient, while the second segment manipulates the attribute "HT_COEFF_GIV" depending on the vapor content in the WM. This attribute is a Boolean value and determines whether the program calculates the value of the heat transfer coefficient or not, thus taking the determined value from its own automation. In addition, this ensures that the values from the automation are only valid in the two-phase region.

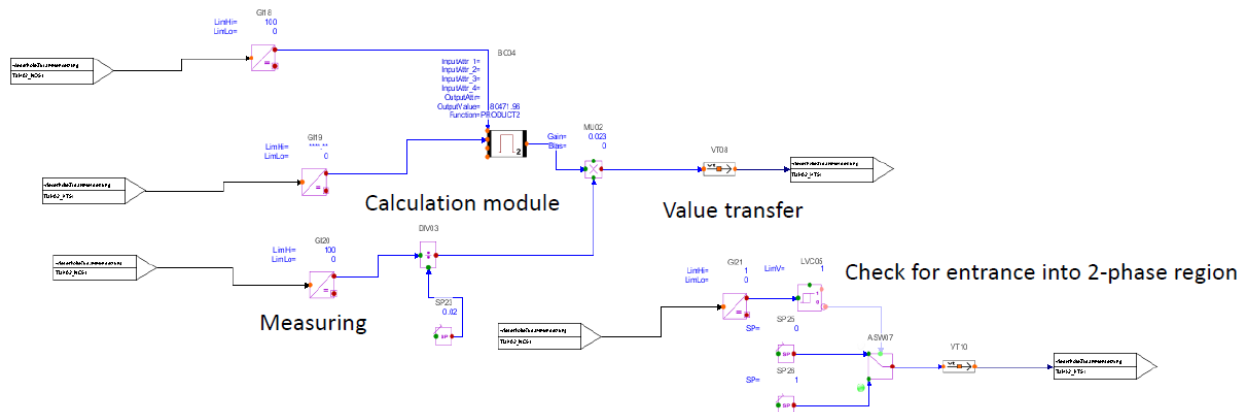


Figure 4: Exemplary automation for the calculation of the heat transfer coefficient with equation (6), adapted from [7]

The second part of the automation is basically needed in all three approaches for the precoolers. There are thermo-hydraulic calculation nodes in this heat exchanger, in which the fluid is in the gaseous state, and therefore, the automation shall execute the standard calculation.

It is pointed out in the documentation of APROS still that with automation, which forms component chains, the order of the computation is of importance. It is determined in the preparation phase of the experiment. Thus, the optimal order may not be observed in the case of loops occurring in the automation. This circumstance may show in the calculation results. Due to the calculation time, the simulation should consist of a minimum of necessary components. If measurement components are in use, they should be set fine enough via the time constant for the internal filter.

In the second case, a self-designed user component created in the model library is used. The parameter-specific inputs and outputs are created for this under a specific name in the configuration, while the calculation basis is given by an SCL-code in which the equations and the variables used are defined. The user component uses the same interface at the output as that of the Value Transmitter, shown in Figure 5. This allows the component to be connected directly to the WM, which means that the transmission component becomes obsolete, and the SCL-code

can directly manipulate the heat transfer coefficient variable. The code is thereby executed at each time step, after the simulation step.

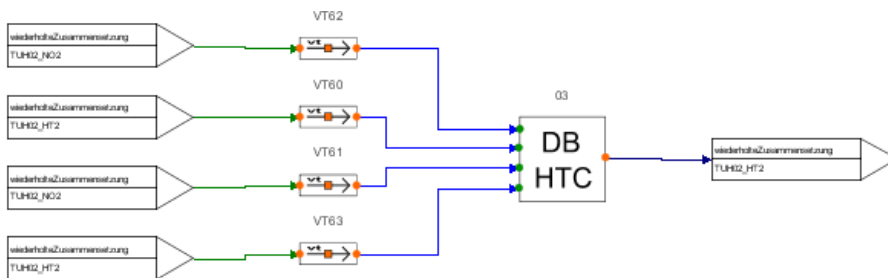


Figure 5: Exemplary SCL-code based user component for the Dittus-Boelter relation according to equation (6), [7]

In the third case, a module called "External Automation" is used. This module accesses an external code to map the equation, which is written in a suitable programming environment (e. g. Visual Studios), either in C or Fortran. This code is called and executed by the component in a DLL file via a shared library. The DLL-file can contain several functions, but the module can only call one of these functions at a certain point of time.

There are some constraints to this method. The parameters necessary for the calculation of the heat transfer coefficient are taken from the calculation level of the process component, and the calculated result is fed back to it. Both the TB and the WM are involved in this process. For each combination of these calculation components, a user component is needed for manipulation, which means that the number of user components must be adapted to the discretization. Due to a high discretization, as it is given, for example, in the process component of the test tube, a high number of the user-defined components is thus necessary, which becomes obvious in Figure 6. In addition, all calculation components involved in the calculation must be drawn on a work surface since otherwise, the necessary connections cannot be laid. This results in a noticeable additional effort for the calculation.

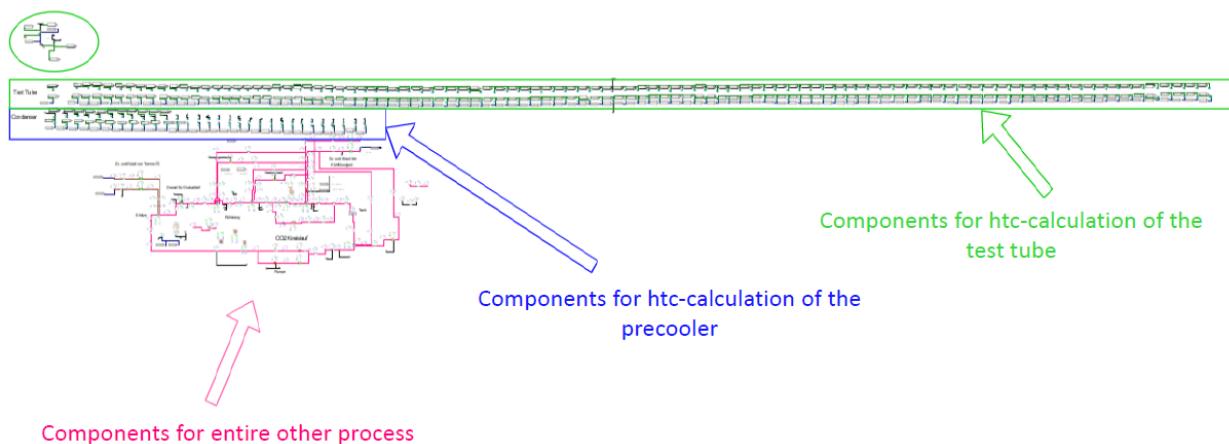


Figure 6: Number of calculation components necessary to manipulate the heat transfer coefficient of the precooler and the test tube in comparison to the entire process, adapted from [7]

5 Results

5.1 Studying the calculation of heat transfer

The biggest amount of work was put into understanding the calculation of heat transfer and “fixing” the unsuitable correlation. Results were already shown in Chapter 4.

An overview of assessed heat transfer correlations is given here:

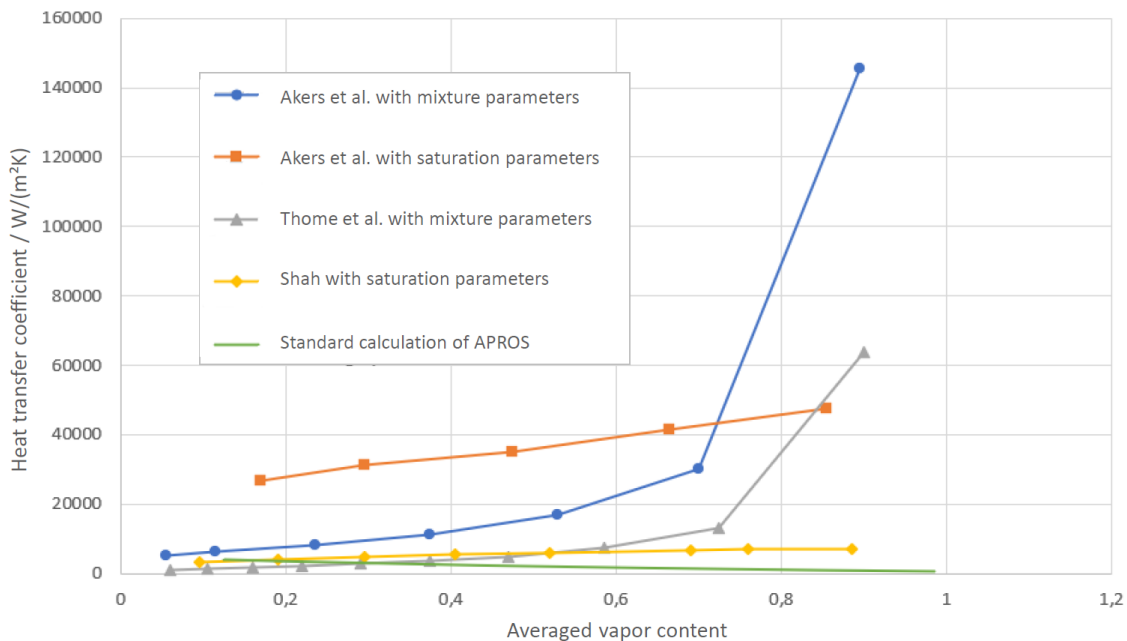


Figure 7: Heat transfer coefficients of different correlations for condensing experiments, correlations from [11], [12], [13]

5.2 Modelling Mod1 test rig - cooling experiments

From the results concerning the test tube when cooling superheated CO₂, it can be seen that there are hardly any differences between the experiments with 66 and 63 bar, except for the fact that the cooling capacity is slightly higher at higher pressure. In the case of the pressure difference, the differences of the parameters occurring in equation (8) are so slight that hardly any change can be seen in the results. A difference becomes apparent only at lower temperatures.

The CO₂-side heat transfer coefficient increases with increasing mass flow and lower temperature, which the Reynolds number's influence can explain. The higher mass flows cause a higher flow velocity, while at lower temperatures, the density of the CO₂ is higher and the dynamic viscosity is lower.

Table 2: Results of cooling experiments

Mass flow	T _{in}	66 bar	63 bar	66 bar	63 bar	66 bar	63 bar
		T _{out}		α- CO ₂ side		Total heat flow	

kg/s	°C	°C		W/(m ² K)		kW	
0.1	120	87.00	86.84	648.43	642.11	4.02	3.99
	60	46.72	46.52	739.70	719.00	2.21	2.15
0.2	180	134.48	134.34	1129.92	1123.60	10.27	10.22
	80	63.34	63.16	1183.47	1161.43	4.64	4.56
0.3	180	139.29	139.15	1565.87	1555.73	13.74	13.67
	80	65.12	64.95	1630.86	1601.30	6.15	6.05
0.4	168	133.60	133.46	1963.02	1950.79	15.53	15.45
	80	66.36	66.20	2047.55	2011.42	7.43	7.32

It can be seen from Table 2 that the small pressure difference of 3 bar has hardly any effect on the performance of the test tube in the case of cooling, and thus the performance differences are minor.

Since the equation (8) of Dittus-Boelter satisfies the conditions of the experiments during cooling within the test tube, the results should be plausible. In the case of cooling in relation to the cooling mixture, the precooler exhibits the same behavior as the test tube. However, the differences between the values at saturation pressures are a trace higher. The required mass flow of the coolant to maintain the desired temperature difference of the CO₂ increases slightly with higher pressure, since the enthalpy difference increases overall as a result. The equation (8) results should give a good representation of reality for the precooler since the given limits are kept.

5.3 Modelling Mod1 test rig - condensing experiments

The test tube results for the experiments of condensing with the standard equation (13) show a completely different course compared to the condensation presented in the literature. The heat transfer coefficient starts at very low values at high vapor content and propagates rapidly as condensation progresses. Thus, especially at the beginning of the process, the low heat transfer coefficient strongly hinders the dissipated heat flow, and the condensation steps turn out to be very small. On the one hand, the slope of the heat transfer coefficient should be exactly the opposite, and, on the other hand, it should not be that high at the high temperatures of the experiments discussed here.

This fact can be explained by equation (13) itself. In the equation, the laminar and turbulent parts, represented by equation (12) and equation (8), are weighted by a smoothing coefficient. This smoothing coefficient depends on the vapor content and a constant. With the default value of this constant of 0.01, the smoothing coefficient depends only on the steam number. This means that only the laminar part of the equation is applied at the beginning of condensation. This part only calculates values between approx. 600 and 640 W/(m²K) over the entire process of condensation. This is why the heat transfer coefficient is so low at the beginning of the process. As the vapor content decreases, the turbulent part of the equation increases, calculating higher values. This leads to the rapid slope in the opposite direction. Accordingly, the equation provided by the software is unsuitable to represent the behavior of condensation inside pipes.

Whether the standard equation (13) is sufficient to represent the behavior of the condensation of CO₂ on the outside of pipes cannot be answered at this point, since no comparative values were found in the literature for this special topic.

However, the results of the self-installed equations regarding the heat transfer coefficient of the test tube all show a significantly better approximation to the behavior of condensation from theory. The heat transfer coefficient decreases along with the vapor content and shows higher values overall due to larger mass flow densities.

However, the equations fed by mixing values from the simulation show a strong slope, especially at high vapor coefficients, which do not appear in the correlations fed by saturation parameters. Since a rather constant behavior of the heat transfer coefficient is required due to the high temperatures, the equations of Thome et al. [12] for saturation parameters from the simulation are chosen here as the most promising possibility since they do not show a sudden increase.

5.4 Finding control parameters to use as a guess for actual operation and determine the most efficient order of experiments

Controller parameters were found:

Figure 8: Controller parameter

PID controller	K_{pr}	T_N in s	T_D in s
Pump - increasing the mass flow	0,02	4	1
Pump - decreasing the mass flow	0,02	10	1
Expansion valve	1,00	150	-
inlet temperature of the CO ₂ at the precooler	1,70	30	-
Mass flow of thermal oil	1,00	100	-
Valve of the precooler-> outlet temperature	0,50	4	0,02
Valve of the precooler -> Vapor content at the outlet	0,10	80	-
Test tube water side valve	10,00	10	-
Condenser water side valve	1,50	50	0,50
Subcooler water side valve	1,00	165	-

However, the time spans not only depend on the system but also on controlling speed (namely controller parameters).

5.5 See the influence of water in comparison to coolant (35% MEG) in case the TU Wien building department switches operation without giving notice

As expected, the results show a significant influence of coolant usage instead of pure water, see Figure 9.

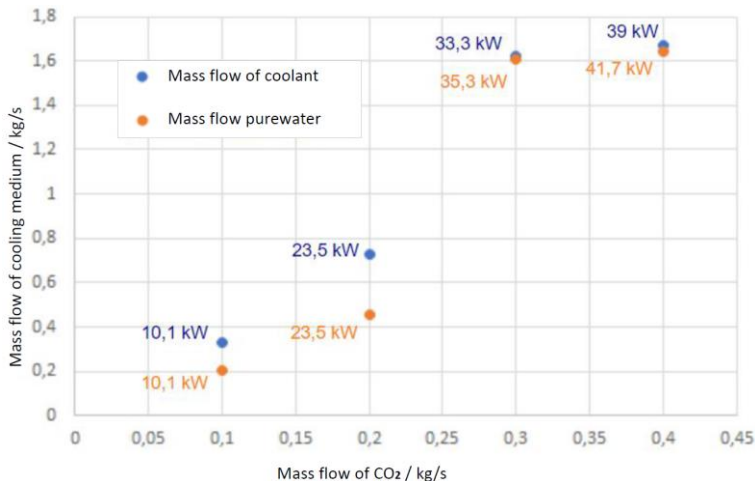


Figure 9: Required cooling mass flows at the precooler to achieve defined temperature differences when cooling CO₂ at 66 bar

Table 3: Results of the precooler with coolant and Section EP

CO ₂		66 bar	63 bar	66 bar	63 bar	
Mass flow CO ₂	T _{in}	T _{out}	Mass flow coolant		Total heat load	
kg/s	°C	°C	kg/s		kW	
0.1	140	60	0.328	0.306	10.093	9.897
0.2	180	80	0.727	0.693	23.537	23.244
0.3	174/175	80	1.621	1.632	33.295	33.200
0.4	162/163	80	1.671	1.687	39.023	38.929

Table 4: Results of the precooler with pure water and Section EP

CO ₂		66 bar	63 bar	66 bar	63 bar	
Mass flow CO ₂	T _{in}	T _{out}	Mass flow coolant		Total heat load	
kg/s	°C	°C	kg/s		kW	
0.1	140	60	0.206	0.194	10.071	9.897
0.2	180	80	0.454	0.433	23.533	23.247
0.3	180	80	1.607	1.485	35.300	34.866
0.4	168	80	1.646	1.534	41.702	41.164

5.6 Determine how long it takes to reach thermodynamic equilibrium

APROS predicted 15 – 40 min periods for reaching the equilibrium; depending on the change of conditions. After conducting the experiments, this fits the actual conditions very well. However, the time spans depend not only on the system but also on controlling speed (namely controller parameters).

5.7 Modeling of CO₂ with RP or EP

In the cooling experiments, the CO₂ is modeled with the help of two different sections. It was noticed that the calculation time increases tenfold with section "RP". Since the calculation and thus the time expenditure is enormous anyway due to the numerous components, this alternative is suitable only for experiments, which can run automatically without manual interferences. Furthermore, the results differ, if then only minimally from those with Section "EP". Therefore, for adjustments of the simulation model, one should use section "EP".

Summary and Conclusion

From our efforts understanding the software, we can draw the following conclusions:

- APROS is not as powerful for CO₂ cycle-simulations as for water/steam cycles since for CO₂, only the 3-equation model is available.
- Predefined heat transfer calculation is difficult to understand, not well documented, and might misrepresent heat transfer of CO₂ as known from the literature.
- Implementing user-defined equations is possible but cumbersome.
- However, the authors gained a tremendous amount of knowledge about the inner workings of APROS which is summarized in [7] and this deliverable.

The next steps include comparing the simulation inputs (e. g. controller parameters) to actually used controllers and comparing the new results to our Mod1 experiments. Based on these results, the decision must be made whether the program's complexity is worth the effort as long as the 6-equation model is not available for CO₂. The results will be published as a Journal paper in case APROS is a suitable tool for sCO₂ power cycle simulation or as a conference paper otherwise.

Literature

- [1] X. Wang, R. Wang, X. Bian, J. Cai, H. Tian, G. Shu, X. Li e Z. Qin, «Review of dynamic performance and control strategy of supercritical CO₂ Brayton cycle,» *Energy and AI*, 2021.
- [2] Apros development team, «Homogenous Model of APROS,» VTT Technical Research Center, Finland, 2015.
- [3] J. E. A. Slide, «Containment model library of the Apros process simulation software: an overview of development and validation work,» *Progress in Nuclear Energy*, pp. 28-45.
- [4] F. Alobaid, R. Starkloff, S. Pfeiffer, K. Karner, B. Epple e F. Alobaid, «A comparative study of different dynamic process simulation codes for combined cycle power plants - part A: Part loads and off-design operation,» *Fuel*, 2015.
- [5] J. Kurki, *Simulation of thermal hydraulics at supercritical pressures with APROS, thesis*, Helsinki: Helsinki University of Technology, 2008.
- [6] R. Span e W. Wagner, «A New Equation of State for Carbon Dioxide Covering the Fluid Region from the Triple-Point Temperature to 1100 K at Pressures up to 800 MPa,» *Journal of Physical and Chemical Reference Data*, pp. 1509-1596, 1996.
- [7] P. Bukovcan, *Dynamische Simulation und Analyse des Wärmeübergangs eines Kohlenstoffdioxid Kreisprozesses*, diploma thesis, Wien, 2021.
- [8] F. Dittus e L. Boelter, «Heat transfer in automobile radiators of the tubular type,» *International Communications in Heat and Mass Transfer*, pp. 3-22, 1985.
- [9] J. Chen, «Correlation for Boiling Heat transfer to Saturated Fluids in Convective Flow,» *Ind. Eng. Chem. Proc. Des. Dev.*, 1966.
- [10] J. Collier e J. Thome, *Convective Boiling and Condensation*, Oxford: Clarendon Press, 1994.
- [11] Z. Zhang et al., «CO₂ condensation heat transfer coefficient and pressure drop in a mini-channel space condenser,» *Experimental Thermal and Fluid Science*, 2013.
- [12] J. R. Thome, J. El Hajal e A. Cavallini, «Condensation in horizontal tubes, part 2: new heat transfer model based on flow regimes,» *International Journal of Heat and Mass Transfer*, 2003.
- [13] M. Shah, «Prediction of heat transfer during condensation of carbon dioxide in channels,» *Applied Thermal Engineering*, 2016.
- [14] J. H. Park, S. W. Bae, H. S. Park, J. E. Cha e M. H. Kim, «Transient analysis and validation with experimental data of supercritical CO₂ integral experiment loop by using MARS,» *Energy*, pp. 1030-1043, 2018.
- [15] X. Li, G. Shu, H. Tian, L. Shi e X. Wang, «Dynamic modeling of CO₂ transcritical power cycle for waste heat recovery of gasoline engines,» *Energy Procedia*, pp. 1576-1581, 2017.
- [16] G. Klemencic, A. Werner, M. Haider, H. Leibinger, T. Fellner, N. Steinschaden, T. Bergthaller e T. Nowack, «Design and dynamic simulation of a 200 kWth laboratory sCO₂-test rig,» in *2nd European sCO₂ Conference 2018*, Essen, 2018.
- [17] H. Ding, W. Li, C. Duan, H. Xu, P. Ding, Y. Zhang e G. Hong, «A thermal-hydraulic analysis model of printed circuit heat exchangers for system simulation using Modelica,» *Journal of Nuclear Science and technology*, 2021.